C. R. Acad. Sci. Paris, Ser. I 348 (2010) 1033–1038

Contents lists available at ScienceDirect

C. R. Acad. Sci. Paris, Ser. I

www.sciencedirect.com

Numerical Analysis

Symplectic schemes for highly oscillatory Hamiltonian systems with varying fast frequencies ☆

Intégrateurs symplectiques pour des systèmes Hamiltoniens hautement oscillants avec fréquences rapides variables

Matthew Dobson [a], Claude Le Bris [a,c], Frédéric Legoll [b,c]

[a] *CERMICS, École des Ponts ParisTech, 77455 Marne-La-Vallée cedex 2, France*
[b] *Institut Navier, LAMI, École des Ponts ParisTech, 77455 Marne-La-Vallée cedex 2, France*
[c] *INRIA Rocquencourt, MICMAC project, domaine de Voluceau, B.P. 105, 78153 Le Chesnay cedex, France*

ARTICLE INFO

Article history:
Received 15 May 2010
Accepted after revision 17 August 2010
Available online 15 September 2010

Presented by Olivier Pironneau

ABSTRACT

We derive symplectic integrators for a class of highly oscillatory Hamiltonian systems. Our approach is based upon a two-scale expansion of the solution to the Hamilton–Jacobi equation associated to the original dynamics. This Note presents an extension of the approach previously introduced in Le Bris and Legoll (2007, 2010) [10,11] to the case where the fast frequencies of the system, instead of being constant, explicitly depend on the slow degrees of freedom.

RÉSUMÉ

Nous dérivons des intégrateurs symplectiques pour une classe de systèmes Hamiltoniens hautement oscillants. L'approche est basée sur un développement à deux échelles de la solution de l'équation de Hamilton–Jacobi associée à la dynamique originale. Cette Note présente une extension des techniques précédemment introduites dans Le Bris et Legoll (2007, 2010) [10,11] au cas où les fréquences rapides du système ne sont plus constantes, mais dépendent des variables lentes.

Version française abrégée

Nous continuons notre entreprise [10,11] de dérivation d'intégrateurs numériques symplectiques pour une classe de systèmes Hamiltoniens hautement oscillants. L'approche est basée sur une réécriture de la dynamique Hamiltonienne en terme d'équation de Hamilton–Jacobi. La solution de cette équation est alors formellement développée en puissances de ε (taille des fréquences les plus rapides présentes dans le système) à la manière d'un développement à deux échelles en homogénéisation. Le schéma numérique est ensuite obtenu en revenant dans les variables originales.

La classe de systèmes Hamiltoniens (2) que nous savons traiter par notre approche est celle où la partie rapide est une partie harmonique, ce qui a pour conséquence une périodicité de la solution de l'équation de Hamilton–Jacobi et permet le développement de cette solution. Dans [10,11], nous avions considéré le cas de fréquences rapides constantes. La présente

☆ This work was supported in part by the NSF Mathematical Sciences Postdoctoral Research Fellowship, by the INRIA under the grant "Action de Recherche Collaborative" HYBRID, and by the Agence Nationale de la Recherche, under grant ANR-09-BLAN-0216-01 (MEGAS).

E-mail addresses: dobsonm@cermics.enpc.fr (M. Dobson), lebris@cermics.enpc.fr (C. Le Bris), legoll@lami.enpc.fr (F. Legoll).

1631-073X/$ – see front matter
doi:10.1016/j.crma.2010.08.005

Note a pour but d'étendre l'étude de [10,11] au cas où les fréquences rapides *dépendent* des variables lentes du système. Cette extension, intéressante pour beaucoup de situations importantes en pratique, requiert une substantielle adaptation de l'approche. Ce travail est aussi l'occasion de revisiter un certain nombre de questions laissées ouvertes dans nos précédentes études sur le cas de fréquences constantes. En particulier, alors qu'il est bien connu que les approches basées sur le formalisme Hamilton–Jacobi présentent l'inconvénient de demander le calcul de dérivées d'ordre élevé des potentiels présents dans le Hamiltonien (2) (ce qui peut s'avérer limitant pour certaines situations pratiques), nous démontrons que l'approche garde tous ses avantages quand on utilise des approximations par différences finies de ces dérivées.

Nos résultats numériques, obtenus sur des systèmes modèles présentant les caractéristiques importantes de systèmes d'intérêt pratique, démontrent, en comparaison d'autres approches standards utilisées sur ce type de systèmes, que notre approche : (a) présente moins de résonances, (b) a une efficacité en terme de coût comparable (quoique légèrement inférieure), et (c) permet, parce qu'elle n'élimine aucun des degrés de liberté rapides, de rendre compte plus fidèlement des propriétés qualitatives du système global qui dépendent de ces degrés rapides. Nos résultats numériques et notre étude seront complétés dans [4].

1. Introduction

This work is a follow-up of our previous works [10,11]. Our purpose is to construct symplectic numerical integrators for the following class of highly oscillatory Hamiltonian systems:

$$\frac{\mathrm{d}\breve{q}}{\mathrm{d}t} = \frac{\partial H_\varepsilon}{\partial \breve{p}}(\breve{q},\breve{p}), \quad \frac{\mathrm{d}\breve{p}}{\mathrm{d}t} = -\frac{\partial H_\varepsilon}{\partial \breve{q}}(\breve{q},\breve{p}), \tag{1}$$

$$H_\varepsilon(\breve{q}_1,\breve{q}_2,\breve{p}_1,\breve{p}_2) = \frac{\breve{p}_1^T\breve{p}_1}{2} + \frac{\breve{p}_2^T\breve{p}_2}{2} + \widetilde{V}(\breve{q}_1,\breve{q}_2) + \big(\Omega(\breve{q}_1)\big)^2\frac{\breve{q}_2^T\breve{q}_2}{2\varepsilon^2}, \tag{2}$$

where we denote $\breve{q} = (\breve{q}_1,\breve{q}_2) \in \mathbb{R}^s \times \mathbb{R}^f$ and $\breve{p} = (\breve{p}_1,\breve{p}_2) \in \mathbb{R}^s \times \mathbb{R}^f$, the upper indices s and f designate the slow and fast variables respectively, and where $\widetilde{V}$ is an interaction potential independent of ε and bounded from below. In contrast to [10] where the frequency Ω was held constant, we consider the case of practical interest where $\Omega(q_1)$ depends on the slow variables. We assume the frequency is a scalar and is bounded from below, $\Omega(q_1) \geqslant c > 0$ for all q_1. The initial conditions for (1) scale with ε so that the initial energy is bounded independently of ε. Since ε, which models the fastest frequencies of the system, is small, direct discretization is expensive.

This type of Hamiltonian system has already been studied in many works [1,2,7,9]. See [3,11] for a short review of the literature, and [9, Chap. XIII and XIV] for a general overview.

As in [10,11], our approach is based on the Hamilton–Jacobi formalism which gives a symplectic scheme by construction (see [5]). However, the dependence of Ω on the slow variables introduces substantial new difficulties, which will be described in Section 2. We additionally address some issues left outstanding by the previous works and provide further analysis of the proposed integrators as compared to other standard integrators. In particular, we successfully replace the high-order derivatives that naturally arise from the Hamilton–Jacobi formalism with finite differences within the generating function, preserving the symplecticity and simplifying the implementation of the scheme.

Our numerical tests demonstrate that the derived method has very good error performance with respect to resonances. Its computational efficiency is comparable, though slightly lower due to implicitness, to established approaches for small ε (such as 10^{-4}) and does not break down as $\varepsilon \to 0$. The fact that we do not eliminate the fast variables allows us to capture qualitative properties depending on these degrees of freedom, such as exchange of fast actions within the system. We note that the algorithm presented has many possible variants based on the choice of approximations of the generating function. Among the possible variants are those that reduce to the algorithms given in [11] whenever Ω is constant. We provide more details in [4].

2. Formalism

The principle behind our approach is to work within the Hamilton–Jacobi framework which yields integrators that are automatically symplectic. Let $\bar{S}_\varepsilon(t,q,P)$ be the solution to

$$\partial_t \bar{S}_\varepsilon = H_\varepsilon(q + \partial_P \bar{S}_\varepsilon, P), \quad \bar{S}_\varepsilon(0,q,P) = 0.$$

For all (q,p,t), it is known that $(Q(t),P(t))$ implicitly defined by

$$p = P(t) + \frac{\partial \bar{S}_\varepsilon}{\partial q}\big(t,q,P(t)\big), \qquad Q(t) = q + \frac{\partial \bar{S}_\varepsilon}{\partial P}\big(t,q,P(t)\big), \tag{3}$$

are solutions to (1) with initial conditions (q,p). We will construct an approximation to $\bar{S}_\varepsilon$ by expanding in powers of ε and deriving a numerical integrator from the approximate solution. Before applying the Hamilton–Jacobi formalism, we make the symplectic change of variables [9, p. 555]

$$q_1 = \breve{q}_1, \qquad p_1 = \breve{p}_1 - \frac{\nabla\Omega(\breve{q}_1)}{2\Omega(\breve{q}_1)}\breve{q}_2^T\breve{p}_2, \qquad q_2 = \frac{\sqrt{\Omega(\breve{q}_1)}}{\sqrt{\varepsilon}}\breve{q}_2, \qquad p_2 = \frac{\sqrt{\varepsilon}}{\sqrt{\Omega(\breve{q}_1)}}\breve{p}_2, \tag{4}$$

which gives:

$$H_2(q_1,q_2,p_1,p_2)=\frac{1}{2}\left(p_1+\frac{\nabla\Omega(q_1)\,q_2^T p_2}{2\Omega(q_1)}\right)^2+\frac{\Omega(q_1)}{2\varepsilon}\left(p_2^T p_2+q_2^T q_2\right)+\widetilde{V}\left(q_1,\frac{\sqrt{\varepsilon}}{\sqrt{\Omega(q_1)}}q_2\right).$$

We neglect part of the slow momentum term and arrive at

$$H_2^{\text{simp}}(q_1,q_2,p_1,p_2)=\frac{1}{2}p_1^T p_1+\frac{\Omega(q_1)}{2\varepsilon}\left(p_2^T p_2+q_2^T q_2\right)+V(q_1,\sqrt{\varepsilon}q_2),$$

where

$$V(q_1,q_2)=\widetilde{V}\left(q_1,\frac{1}{\sqrt{\Omega(q_1)}}q_2\right) \tag{5}$$

and where we note that the term we neglected is $O(\varepsilon)$. This will introduce only small errors for times of length $O(\varepsilon)$, and we will observe in our numerical experiments that this change does not introduce errors larger than $O(\varepsilon)$ in the energy, the adiabatic invariant, or the exchange of fast actions (9) over times of length $O(\varepsilon^{-2})$. When we discuss error in energy, we always refer to the energy computed from the unmodified Hamiltonian H_ε in (2).

We now introduce the fast time

$$\sigma(t)=\frac{1}{\varepsilon}\int_0^t \Omega\big(q_1(s)\big)\,\mathrm{d}s$$

and consider the time-dependent change of variables $(q_2,p_2)\mapsto(\tilde{x},\tilde{y})$ defined by

$$q_2=\tilde{x}\cos\big(\sigma(t)\big)+\tilde{y}\sin\big(\sigma(t)\big),\qquad p_2=-\tilde{x}\sin\big(\sigma(t)\big)+\tilde{y}\cos\big(\sigma(t)\big).$$

Note that the dynamics on $(q_1,\tilde{x},p_1,\tilde{y})$ includes a *memory term* due to σ. Rather than operate on a system with memory, we consider σ as an additional variable and add the corresponding conjugate variable $I=\frac{1}{2}(\tilde{x}^T\tilde{x}+\tilde{y}^T\tilde{y})$. In this way, we extend to a higher-dimensional autonomous dynamics which turns out to be a Hamiltonian dynamics with energy

$$H_3(q_1,\tilde{x},\sigma,p_1,\tilde{y},I)=\frac{1}{2}p_1^T p_1+V\big(q_1,\sqrt{\varepsilon}(\tilde{x}\cos\sigma+\tilde{y}\sin\sigma)\big)+I\frac{\Omega(q_1)}{\varepsilon}.$$

We write the Hamilton–Jacobi equation associated to H_3 and then rescale the variables I, $\tilde{x}$ and $\tilde{y}$,

$$a=\frac{I}{\varepsilon},\qquad x=\frac{\tilde{x}}{\sqrt{\varepsilon}}\quad\text{and}\quad y=\frac{\tilde{y}}{\sqrt{\varepsilon}},$$

so that all variables are of the same order. The Hamilton–Jacobi equation becomes

$$\begin{aligned}\partial_t S_\varepsilon(t,q_1,x,\Sigma,P_1,Y,a)&=H_3\left(q_1+\partial_{P_1}S_\varepsilon,\sqrt{\varepsilon}\left(x+\frac{1}{\varepsilon}\partial_Y S_\varepsilon\right),\Sigma,P_1,\sqrt{\varepsilon}Y,\varepsilon a-\partial_\Sigma S_\varepsilon\right)\\&=\frac{1}{2}P_1^T P_1+V\big(q_1+\partial_{P_1}S_\varepsilon,(\varepsilon x+\partial_Y S_\varepsilon)\cos\Sigma+\varepsilon Y\sin\Sigma\big)\\&\quad+\Omega(q_1+\partial_{P_1}S_\varepsilon)\left(a-\frac{1}{\varepsilon}\partial_\Sigma S_\varepsilon\right).\end{aligned} \tag{6}$$

We make the two-scale ansatz

$$S_\varepsilon(t,q_1,x,\Sigma,P_1,Y,a)=S_0(t,q_1,P_1,a)+\sum_{k=1}^{\infty}\varepsilon^k S_k\left(t,\Sigma-\frac{1}{\varepsilon}\tau(t,q_1,P_1,a),q_1,x,\Sigma,P_1,Y,a\right)$$

using a fast time τ, which will be solved for in the resulting equations giving $\tau(t,q_1,P_1,a)=t\Omega(q_1+\frac{t}{2}P_1)$. To close the resulting hierarchy of equations, we assume that $S_k(t,\beta,q_1,x,\gamma,P_1,Y,a)$ is 2π periodic in γ (consistent with the fact that the generating function of a harmonic oscillator is periodic in time), and we also assume the existence of a transport structure, $\Sigma-\frac{1}{\varepsilon}\tau$, on the fast time τ. We insert this ansatz into (6) and expand the equation in powers of ε. Equating powers of ε and solving for the first three orders S_0, S_1, and S_2 (where we find $S_1=0$), we take the following approximate generating function

$$\begin{aligned}S_\varepsilon=t\Big[&\frac{1}{2}P_1^T P_1+V\left(q_1+\frac{t}{2}P_1,0\right)+a\Omega\left(q_1+\frac{t}{2}P_1\right)\Big]+O\big(t^3\big)+\varepsilon^2\Big[\frac{\nabla_2 V(q_1+tP_1,0)}{\Omega(q_1+tP_1)}(x\sin\Sigma-Y\cos\Sigma)\\&-\frac{\nabla_2 V(q_1,0)}{\Omega(q_1)}\Big(x\sin\Big(\Sigma-\frac{t}{\varepsilon}\Omega\Big(q_1+\frac{t}{2}P_1\Big)\Big)-Y\cos\Big(\Sigma-\frac{t}{\varepsilon}\Omega\Big(q_1+\frac{t}{2}P_1\Big)\Big)\\&+\frac{t}{4}\big(x^T\nabla_{22}V(q_1,0)x+Y^T\nabla_{22}V(q_1,0)Y\big)\Big]+O\big(\varepsilon^2 t\big)+O\big(\varepsilon^3\big).\end{aligned} \tag{7}$$

This choice is consistent with the regime $\varepsilon \ll t \ll \varepsilon^{1/3}$. Note that we include a portion of the $O(\varepsilon^2 t)$ term in order to reproduce the exchange of fast actions (see Fig. 2 below). The portion neglected from the $O(\varepsilon^2 t)$ term involves only lower-order contributions to the slow variables, and we find after testing that we satisfactorily capture the exchange of fast actions without including this term.

We now replace the derivatives of V in (7) with finite differences so that the algorithm only requires computing the value and first derivatives of the slow potential V. There is no unique way to make this replacement. One possible approximation of the generating function is

$$\begin{aligned} S_{\varepsilon,\mathrm{FD}} = t\left[\frac{1}{2}P_1^T P_1 + V\left(q_1 + \frac{t}{2}P_1, 0\right) + a\Omega\left(q_1 + \frac{t}{2}P_1\right)\right] \\ + \varepsilon\frac{V(q_1 + tP_1, \varepsilon(x\sin\Sigma - Y\cos\Sigma)) - V(q_1 + tP_1, 0)}{\Omega(q_1 + tP_1)} \\ + \varepsilon\frac{V(q_1, 0) - V[q_1, \varepsilon(x\sin(\Sigma - \frac{t}{\varepsilon}\Omega(q_1 + \frac{t}{2}P_1)) - Y\cos(\Sigma - \frac{t}{\varepsilon}\Omega(q_1 + \frac{t}{2}P_1)))]}{\Omega(q_1)} \\ + \frac{t}{4}\big[V(q_1, \varepsilon x) - 2V(q_1, 0) + V(q_1, -\varepsilon x) + V(q_1, \varepsilon Y) - 2V(q_1, 0) + V(q_1, -\varepsilon Y)\big]. \end{aligned} \tag{8}$$

Note that we have not changed the order of accuracy by making this replacement. Substituting into (3), we arrive at our algorithm, which we denote as $S_{\varepsilon,\mathrm{FD}}$ in the figures.

3. Numerical tests

We provide numerical tests on both a scalar and a vectorial test case. We compare our algorithm to the Impulse [8,12] and Mollify [6] algorithms. Both algorithms follow a kick/oscillate/kick pattern. They incorporate the slow forces, which come from the potential $\widetilde{V}$, only at the "kick" steps, which are separated by a macro-time step that is large with respect to the shortest period in the solution. This time step is typically larger than ε. For the "oscillate" step, these methods integrate the fast forces, which come from the potential $\frac{\Omega(\check{q}_1)^2}{2\varepsilon^2}\check{q}_2^2$, using a stepsize that is small with respect to ε. These algorithms are designed to minimize the number of evaluations of the slow forces, with the assumption that the "oscillate" step is cheaper, or comparable in cost, to a single evaluation of the slow forces. In our tests, we have used the Verlet scheme for the "oscillate" step in both the Impulse and Mollify algorithms. In each figure, we indicate the stepsize used in this inner integration (for example, $\varepsilon/40$ or $\varepsilon/80$ in Fig. 1(d)).

In Fig. 1, we consider a scalar test case with slow potential

$$V(q_1, q_2) = q_1^4 + q_2 q_1^2 + q_2^2, \qquad q_1 \in \mathbb{R},\ q_2 \in \mathbb{R},$$

and frequency

$$\Omega(q_1) = \sqrt{1 + q_1^2}.$$

Note that these are specified in the (q, p) variables. The original potential $\widetilde{V}$ can be found using (5). For these computations, the chosen initial conditions are $\check{q}_1 = \check{q}_2 = 0$ and $\check{p}_1 = \check{p}_2 = 1$ for all three algorithms, which gives the initial energy $H_\varepsilon = 1$, independent of ε.

We first run a simulation over very long times to check that there is no spurious drift in the energy. Note that energy preservation for symplectic schemes is typically proven in the limit $h/\varepsilon \to 0$; however, we consider here $h = 0.02$, $\varepsilon = 0.001$ so energy preservation is not theoretically guaranteed. We run the Impulse, Mollify, and $S_{\varepsilon,\mathrm{FD}}$ algorithms (see Fig. 1(a)–(c)) to time $T = 10^6$. We observe no drift in either Mollify or $S_{\varepsilon,\mathrm{FD}}$. In the Impulse algorithm, the energy varies greatly, due to the resonance effects which are discussed below. For $S_{\varepsilon,\mathrm{FD}}$, the energy plotted here is computed using H_ε by transforming the numerical trajectory given by (3)–(8) back to the original variables using (4).

Fig. 1(d) displays the maximum relative error in energy to time $T = 10^4$,

$$\mathrm{err} = \max_{t\in[0,10^4]} \frac{|H_\varepsilon(t) - H_\varepsilon(0)|}{H_\varepsilon(0)},$$

versus the computational cost which is measured by the total number of evaluations of the slow forces. The figure is produced by holding $\varepsilon = 10^{-4}$ fixed and varying the stepsize. As the stepsize decreases, the computational cost increases. We see that, for fewer than 10^8 force evaluations, the $S_{\varepsilon,\mathrm{FD}}$ algorithm is more efficient than Impulse due to the lack of resonances. The algorithm is more expensive than Mollify but exhibits fewer effects of resonances. The error in the $S_{\varepsilon,\mathrm{FD}}$ algorithm saturates at the level $O(\varepsilon)$, due to neglecting a term in forming H_2^{simp}. The error saturation in Impulse and Mollify is due to the choice of inner integration stepsize (as shown by the two Impulse curves), and in the limit of exact inner integration one expects $O(h^2)$ convergence as $h \to 0$ with ε fixed.

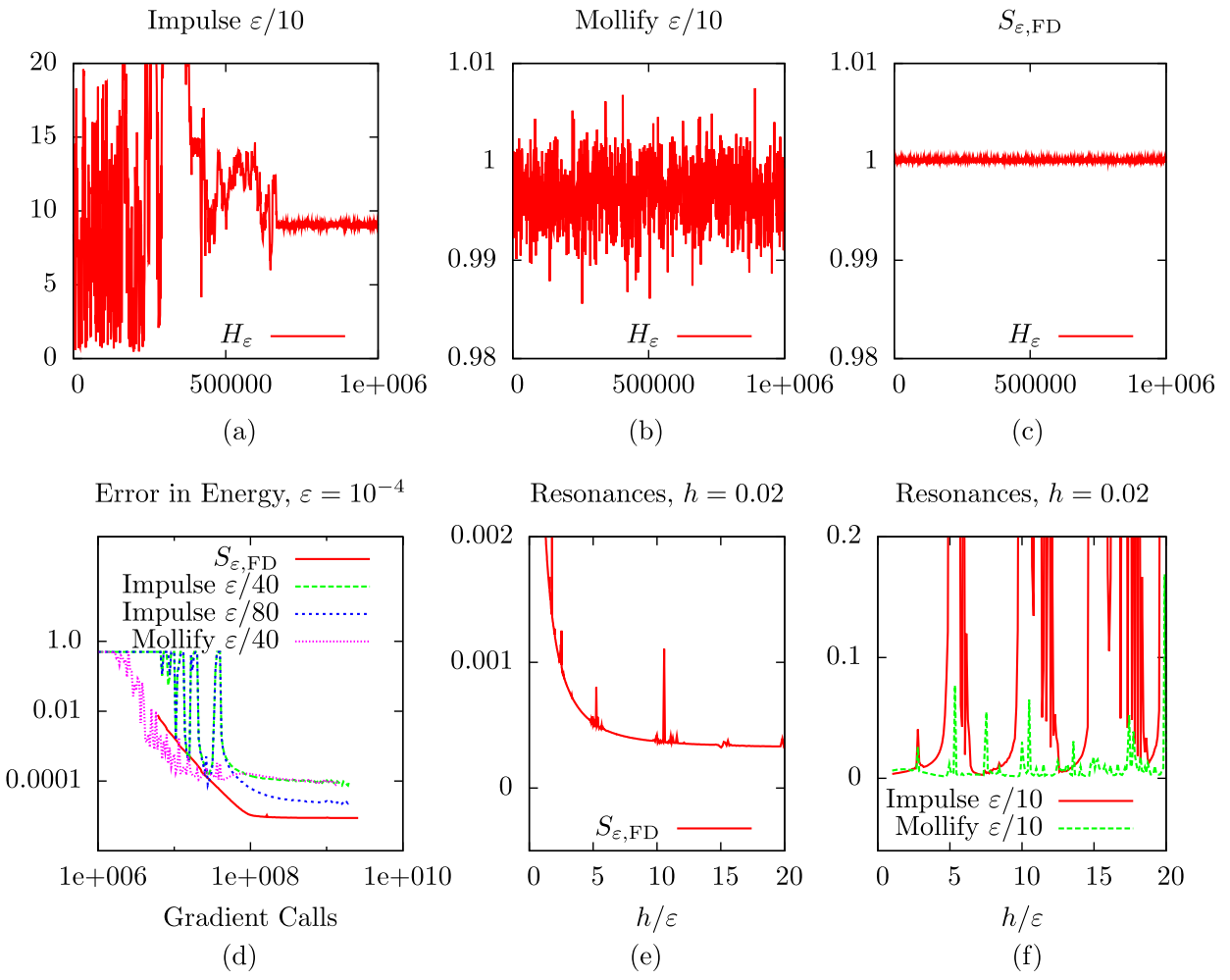

Fig. 1. (a)–(c) Long-time energy preservation of the Impulse, Mollify, and $S_{\varepsilon,\mathrm{FD}}$ algorithms over the long time interval $[0, T]$ where $T = 10^6 = \varepsilon^{-2}$, for $h = 0.02$ (the $\varepsilon/10$ after Impulse and Mollify indicates that the stepsize $\varepsilon/10$ was used in the inner integration to propagate using the fast potential, $\frac{\Omega(\check{q}_1)^2}{2\varepsilon^2}\check{q}_2^2$). For this choice of parameters, Impulse gives a qualitatively wrong solution due to resonances. (d) Comparison of the computational efficiency of the three algorithms: error in the energy is plotted against the number of calls to the slow forces. For a given stepsize h, the algorithm proposed here is more computationally expensive and more accurate. (e) Resonance plot for the proposed algorithm as $\varepsilon \to 0$, with stepsize h held fixed. The algorithm is very robust in this limit. (f) Resonance plot for the Impulse and Mollify algorithms. Note that the vertical scale of plots (e) and (f) differ by a factor of 100.

The final plots in Fig. 1 show resonance plots of the error in energy as a function of the small parameter ε, with the stepsize held fixed. In the $\varepsilon \to 0$ limit, the proposed algorithm is very robust, whereas both Impulse and Mollify exhibit resonances. Note the difference by a factor of 100 in the y-axis scaling of Figs. 1(e) and 1(f).

In order to investigate the accuracy in reproducing features of the fast variables, we now consider a modified version of the Fermi–Pasta–Ulam chain [9, Sec. XIII.2.1], with $q_1 = (q_{1,1}, q_{1,2}, q_{1,3}) \in \mathbb{R}^3$, $q_2 = (q_{2,1}, q_{2,2}, q_{2,3}) \in \mathbb{R}^3$, the standard slow potential, and a fast potential whose frequency depends on the slow variables as in (2). For simplicity, we choose a frequency depending only on the first coordinate $q_{1,1}$ of q_1,

$$\Omega(q_1) = \sqrt{1 + q_{1,1}^2}.$$

Similar to the classical case with constant fast frequencies, in the exact trajectory there is exchange among the actions

$$I_i = \frac{1}{2}\left(q_{2,i}^2 + p_{2,i}^2\right), \tag{9}$$

whereas the sum $I = I_1 + I_2 + I_3$ is nearly conserved, with oscillations of size $O(\varepsilon)$ (see Fig. 2(a) where we used the Verlet algorithm with a very small time step to compute a reference solution). The $S_{\varepsilon,\mathrm{FD}}$ algorithm exhibits a very good qualitative agreement (see Fig. 2(b)).

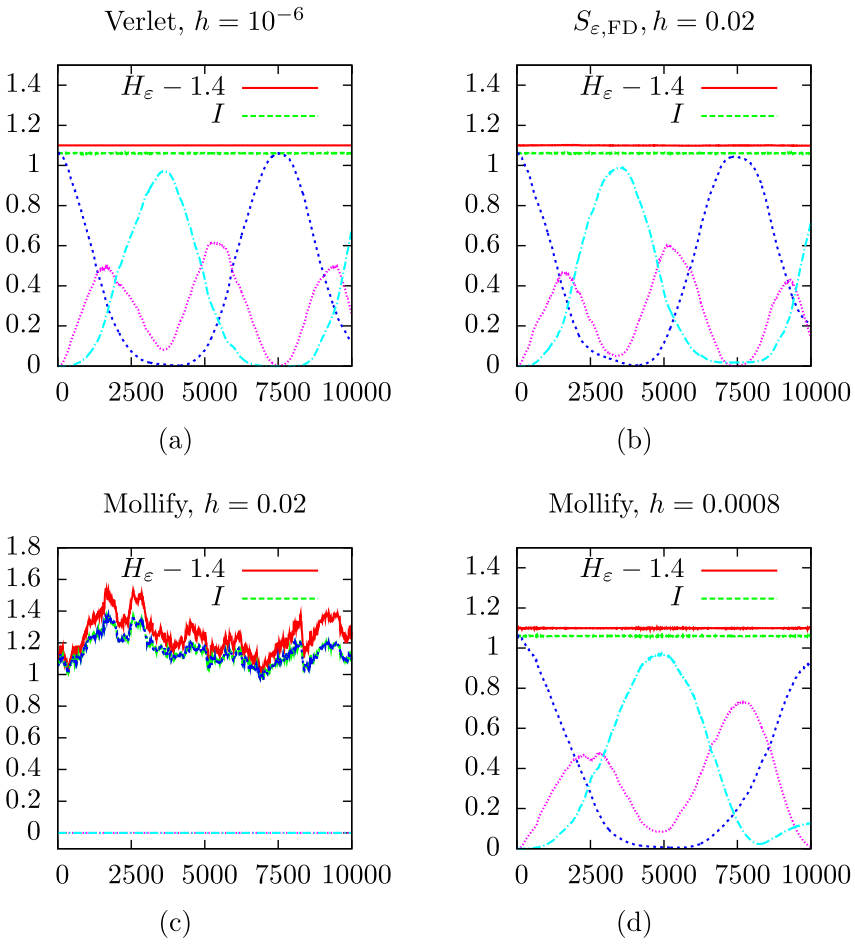

Fig. 2. Exchanges of I_i for a trajectory of the modified FPU problem for (a) Verlet, (b) our algorithm, and (c)–(d) Mollify, for the initial condition $\check{q}_1 = (1, 0, 0)$, $\check{q}_2 = (\varepsilon, 0, 0)$, $\check{p}_1 = \check{p}_2 = (1, 0, 0)$, with $\varepsilon = 10^{-3}$. In (a), (b) and (d), we see that the energy (shifted for convenience) and adiabatic invariant $I = I_1 + I_2 + I_3$ are well-preserved: the maximum error in energy is less than 5.4×10^{-6}, 0.0028 and 0.0066 in (a), (b) and (d) respectively; and the maximum variation in I is 0.0038, 0.0036 and 0.0037 in (a), (b) and (d) respectively. For the stepsize $h = 0.02$, the $S_{\varepsilon,\mathrm{FD}}$ algorithm is stable, whereas Mollify exhibits large oscillations due to resonance effects. We have chosen the stepsize $h = 0.0008$ for Mollify in (d) so that this algorithm and the $S_{\varepsilon,\mathrm{FD}}$ algorithm with $h = 0.02$ have a similar number of slow force evaluations, which we use as a proxy for computational cost for large systems. The $S_{\varepsilon,\mathrm{FD}}$ algorithm exhibits better qualitative agreement with the exchanges present in the reference Verlet integration, even in the case of similar computational costs.

References

[1] F. Bornemann, C. Schuette, Homogenization of Hamiltonian systems with a strong constraining potential, Phys. D 102 (1997) 57–77.
[2] F. Castella, Ph. Chartier, E. Faou, An averaging technique for highly-oscillatory Hamiltonian problems, SIAM J. Numer. Anal. 47 (4) (2009) 2808–2837.
[3] D. Cohen, T. Jahnke, K. Lorenz, Ch. Lubich, Numerical integrators for highly oscillatory Hamiltonian systems: a review, in: A. Mielke (Ed.), Analysis, Modeling, Simulation of Multiscale Problems, in: Mathematics and Statistics Series, Springer, 2006, pp. 553–576.
[4] M. Dobson, C. Le Bris, F. Legoll, Symplectic schemes for highly oscillatory Hamiltonian systems: the homogenization approach beyond the constant frequency case, preprint, arXiv:1008.1030.
[5] K. Feng, Difference schemes for Hamiltonian formalism and symplectic geometry, J. Comp. Math. 4 (1986) 279–289.
[6] B. Garcia-Archilla, J. Sanz-Serna, R. Skeel, Long-time-step methods for oscillatory differential equations, SIAM J. Sci. Comput. 20 (1998) 930–963.
[7] V. Grimm, M. Hochbruck, Error analysis of exponential integrators for oscillatory second-order differential equations, J. Phys. A 39 (2006) 5495–5507.
[8] H. Grubmüller, H. Heller, A. Windemuth, K. Schulten, Generalized Verlet algorithm for efficient molecular dynamics simulations with long range interaction, Mol. Sim. 6 (1–3) (1991) 121–142.
[9] E. Hairer, C. Lubich, G. Wanner, Geometric Numerical Integration, Springer, 2006.
[10] C. Le Bris, F. Legoll, Dérivation de schémas numériques symplectiques pour des systèmes Hamiltoniens hautement oscillants (Derivation of symplectic numerical schemes for highly oscillatory Hamiltonian systems), C. R. Acad. Sci. Paris, Ser. I 344 (2007) 277–282.
[11] C. Le Bris, F. Legoll, Integrators for highly oscillatory Hamiltonian systems: an homogenization approach, Discrete Contin. Dyn. Syst. Ser. B 13 (2) (2010) 347–373.
[12] M.E. Tuckermann, B.J. Berne, G.J. Martyna, Reversible multiple time scale molecular dynamics, J. Chem. Phys. 97 (1992) 1990–2001.